

1 **Moulin density impacts the effect of subglacial**
2 **hydrology on ice dynamics**

3 **B. de Fleurian¹, P. M. Langebroek²**

4 ¹Department of Earth Science, University of Bergen, Bjerkes Centre for Climate Research, Bergen,
5 NORWAY

6 ²NORCE Norwegian Research Centre AS, Bjerkes Centre for Climate Research, Bergen, NORWAY

7 **Key Points:**

- 8 • The density of moulins changes the impact of subglacial water drainage on ice dy-
9 namics.
10 • Localised water inputs to the subglacial hydrological system helps with the sta-
11 bility of the system.

Abstract

The current increase in temperature over Greenland and other glaciated regions allows for more surface melt, which poses the question of the impact of this extra amount of meltwater on ice dynamics. As subglacial hydrology models evolve they are now easier to apply to realistic scenarios to quantify the effect of an increase in melt on the dynamics of glaciers. However, a number of processes linking the surface melt to the water pressure at the base of glaciers are still overlooked in models due to a lack of knowledge or an excess of complexity. Here, we apply a subglacial hydrology model coupled to an ice dynamics model to a synthetic geometry to investigate the impact of moulin distribution on the dynamics of the glacier. Our results show that a sparser distribution of moulins leads to the faster development of the efficient drainage system and greatly slows down the glacier.

Plain Language Summary

As climate warms, a larger amount of meltwater is produced at the surface of ice sheets and glaciers. Most of this water makes its way through cracks and other passageways of the ice to end up at the interface between the glacier itself and the underlying rock. Once at the base of the glacier this water acts as a lubricant and as its pressure increase it has the potential to speed-up the overlying ice. The relationship between ice velocity and water amount is however not straightforward as the drainage system at the base of the glacier can reconfigure and potentially has a large impact on water pressure. Due to this complex interactions, numerical models of subglacial drainage system are needed to get a better idea of the effect of an increase in meltwater production on ice dynamics. Using such a model in a conceptual set-up, we show that reducing the number of injection points into the subglacial drainage system in models can lead to a substantial deceleration of the glacier above.

1 Introduction

Since the first measurement of the impact of meltwater on the dynamics of glaciers in Greenland by Zwally et al. (2002) the question of the long term impact of an increase of Greenland surface melt on its dynamics has been debated within the community. Further observations (e.g., Sole et al., 2013; Meierbachtol et al., 2013; Doyle et al., 2014; Tedstone et al., 2015) have revealed a complex interaction between the amount of runoff at the ice surface and the observed accelerations or lack thereof. A large part of the complexity of the system resides in the way the subglacial water drainage system operates, with the capacity to enhance its efficiency when the water volume injected into the system increases (e.g., Chandler et al., 2013; Andrews et al., 2014). These complex interactions lead to a decoupling between the volume of available runoff water and the subglacial water pressure that drives glacier sliding (Bartholomew et al., 2010; Schoof, 2010; Fitzpatrick et al., 2013; Sole et al., 2013; van de Wal et al., 2015). The complexity of this system warrants the use of fully coupled subglacial hydrology ice dynamics models to evaluate if the increase of meltwater production will have a notable effect on ice dynamics as the temperatures continue to rise (M. Hoffman & Price, 2014; Stevens et al., 2018; Davison et al., 2019).

Important efforts have been made to improve the representation of the subglacial hydrological drainage system in models This lead to the development of a new generation of multi component models able to compute the water pressure at the base of glaciers (e.g. Pimentel et al., 2010; Werder et al., 2013; de Fleurian et al., 2014; M. J. Hoffman et al., 2018). These models have recently been coupled to ice dynamics models in order to investigate the meltwater lubrication feedback on various timescales (Gagliardini & Werder, 2018; de Fleurian et al., 2022), Given the complexity of the system these studies have focused on synthetic designs to isolate the effect of a specific component of the

62 system. Here, we continue on this trend and investigate the impact of the water supply
 63 distribution on the subglacial water pressure and its impact on ice dynamics. This ques-
 64 tion have been under the scope of different studies so far (A. Banwell et al., 2016; Scholzen
 65 et al., 2021) but those studies focused on the effect on subglacial water pressure with-
 66 out taking the final step of assessing the effect on ice dynamics.

67 The distribution intensity and timing of meltwater input to the subglacial drainage
 68 system is controlled by the intensity of the surface melt and the efficiency of the supraglacial
 69 and intraglacial drainage systems. Models are emerging to represent these components
 70 (e.g. A. F. Banwell et al., 2012; Clason et al., 2015; Yang et al., 2022) but the complex-
 71 ity of each subsystem means that there is still no simulations that can introduce in a re-
 72 alistic manner all the component of the system. This is a drawback for the modelling
 73 of subglacial water pressure as the intensity of water input at the base of glaciers has a
 74 large impact on the development of an efficient subglacial drainage system (Colgan et
 75 al., 2011; Bartholomew et al., 2012; Tedesco et al., 2013; de Fleurian et al., 2022) and
 76 hence on the subglacial water pressure. A recent study by Yang et al. (2020) showed that
 77 changing the supraglacial drainage model that was feeding into the subglacial drainage
 78 system did not yield large changes in pressure on timescales longer than a day. Mejia
 79 et al. (2022) drew similar conclusion after monitoring supraglacial drainage catchment
 80 with different characteristics showing again that a change in the supraglacial drainage
 81 can lead to lags in subglacial water peak pressure on the order of a few hours. Here we
 82 focus on longer timescales and investigate the impact of a changes in the distribution of
 83 meltwater input into the subglacial drainage system on a yearly timescale.

84 2 Methods

85 2.1 Model Description

86 In order to investigate the influence of moulins density on the effective pressure and
 87 velocity evolution of glaciers we carry out coupled ice dynamic, subglacial hydrology sim-
 88 ulations within the Ice-sheet and Sea-level System Model (ISSM, Larour et al., 2012).
 89 Within ISSM we use the Double Continuum (DoCo) approximation for the hydrology
 90 model as described in de Fleurian et al. (2014, 2016). The ice flow is then resolved with
 91 a Shallow Shelf Approximation (SSA, Morland & Zainuddin, 1987; MacAyeal, 1989) and
 92 the coupling is achieved through a friction law in which the effective pressure (N), de-
 93 fined as the difference between the water pressure at the bed and the ice overlying pres-
 94 sure, is a key parameter. We elected to use a non-linear friction law described by Schoof
 95 (2005) and Gagliardini et al. (2007) which ties sliding velocities (\vec{u}_b) and basal shear stress
 96 ($\vec{\tau}_b$):

$$97 \quad \vec{\tau}_b + \frac{CN|\vec{u}_b|^{(1/n-1)}}{(|\vec{u}_b| + C^n N^n A_s)^{(1/n)}} \vec{u}_b = 0, \quad (1)$$

98 where C is Iken’s bound (Iken, 1981) which sets the maximum value taken by $\vec{\tau}_b/N$ while
 99 A_s is the sliding parameter without cavitation and n is the rheological exponent in Glen’s
 100 flow law (Glen, 1958) taken here as ($n = 3$).

101 As for most of the model set-up, the subglacial hydrology model version and pa-
 102 rameters used in the present study are exactly the same as the one described in de Fleurian
 103 et al. (2022). As in de Fleurian et al. (2022) the model is initialised with a parabolic func-
 104 tion which resembles a west Greenland land terminating glacier surface elevation. The
 105 glacier is initially 150 km long and 20 km wide with a flat bedrock at an elevation $z_b = 465$
 106 m The surface elevation (z) then follows:

$$107 \quad z_s(x, y) = 4.5 \times \sqrt{x + 4000} + 186 \quad (2)$$

108 The geometry is then relaxed within the coupled model framework to achieve a pseudo
 109 steady-state geometry.

Table 1. Catchment area characteristics for every simulation, the area taken into account for the average catchment area is the area that experiences melt at anytime during the year. The number of moulins corresponds to the number of catchment areas as there is a single moulin per catchment area.

Simulation name	number of moulins	Average catchment area	smallest catchment area
<i>Uniform</i>	844	0.7 km ²	0.1 km ²
<i>Fine</i>	467	1.4 km ²	0.3 km ²
<i>Mid</i>	99	6.5 km ²	1.2 km ²
<i>Coarse</i>	50	13 km ²	2.1 km ²

2.2 Meltwater Forcing

The surface mass balance is applied through an idealised method following Hewitt (2013), where the surface temperature is described at a reference elevation through the length of the melt season (Δ_m), a positive degree day (r_m) at the reference elevations, the day of the year when the melt season starts (t_{spr}) and the duration that the temperature takes to reach its maximum value (Δ_t in days). The reference temperature (T_{ref}) then reads :

$$T_{ref}(t) = \frac{r_m}{\Delta_m} \times \left(\frac{1}{2} \tanh \left(\frac{t - t_{spr}}{\Delta_t} \right) - \frac{1}{2} \tanh \left(\frac{t - (t_{spr} + \Delta_m)}{\Delta_t} \right) \right) \quad (3)$$

From that temperature, the runoff (r) at the surface of our synthetic geometry is computed through a lapse rate (r_s) and a given degree day factor (ddf):

$$r(s, t) = \max \{0, T_{ref}(t) \times (z_s - 465) \times r_s\} \times ddf \quad (4)$$

This setup for the mass balance computation uses the parameters of the reference simulation in de Fleurian et al. (2022) with $\Delta_t=141$ days, a maximum temperature at the reference elevation (r_m/Δ_m) of 5.85 °C and $\Delta_t=10$ days. The major difference here is that the injection in the subglacial hydrology model is slightly different. Our reference simulation (*Uniform* in Table 1) uses the set-up that was previously described where every model node is an injection point in the subglacial hydrology model. However we also use some setup where a smaller number of injection point is used. For simplicity we will further call those injection points moulins even if we do not try to actually model the supraglacial and intraglacial components of the drainage system, implying a direct transfer of surface melt to the base of the glacier at each moulin. The procedure to define those moulins is as follow. First, a given number of nodes are drawn randomly within the nodes of the model that fall within the region that experiences runoff at any time during the year. From this initial draw, we define a Voronoi diagram in which each polygon associated to a given model node represents one drainage basin at the surface of the ice. The moulin for each of those basins is then placed on the lowest elevation node contained in the catchment. From there on, the runoff is integrated over the whole catchment area and the given water discharge is then injected at the location of the moulin through a vertical shaft into the subglacial hydrology model. This procedure insures that for all the simulations the same volume of water is injected in the subglacial drainage system and only the location of the injection changes. Table 1 gives an overview of the different simulations with a few statistics on the catchment areas and number of moulins.

2.3 Ensemble Design

The experiments of de Fleurian et al. (2022) showed that the model presented a physical instability that needed to perform an ensemble of simulations in order to inves-

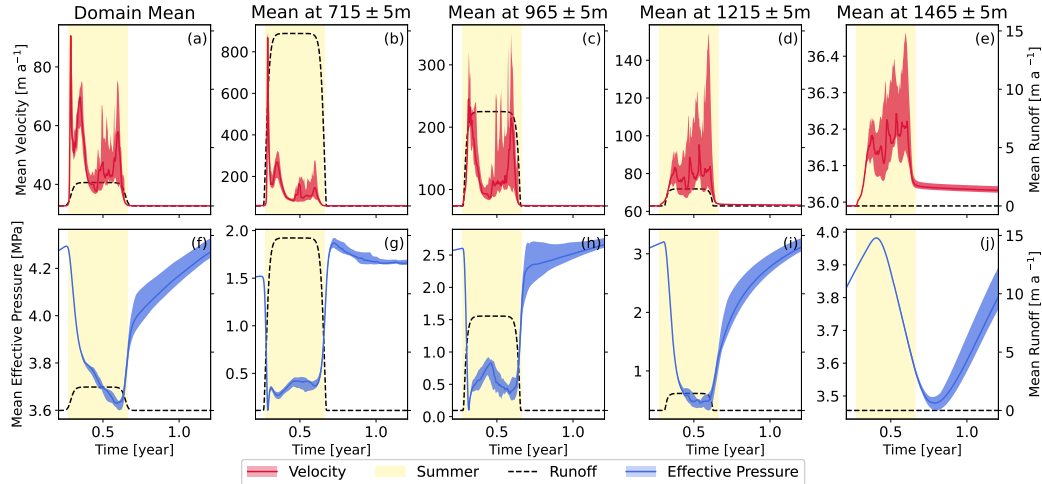


Figure 1. Evolution of velocities (a to e) and effective pressures (f to j) presented as a mean value for the whole domain (a and f) or a given elevation band (b-e and g-j) for the *Uniform* ensemble. The red line and shading show the mean ensemble and spread of the velocity respectively. In the same way, the blue colour represents the effective pressure while the dashed black line is the runoff presented on the right axis. Note that the runoff axis is the same for every plot but that this is not true for the velocity and effective pressure axes. The yellow shading represents the summer period from day 100 to 241.

145 tigate the impact of the different forcings. Here we expect those instability to be similar for the simulations with a large number of moulins (*Uniform* and *Fine* in Table 1),
 146 to cope with this issue we will again perform a ensemble of simulations with this time
 147 only 20 members per ensembles. We use the same method as was used in de Fleurian
 148 et al. (2022) to produce the ensemble with all parameters of the simulations identical but
 149 the starting time which is delayed by one extra second for every simulation.
 150

151 3 Results

152 We take as a reference the *Uniform* simulation in which each model node is an in-
 153 jection point for the subglacial drainage system. In this case, the models counts 844 moulins
 154 that are active at one time or another during the simulation. That translates to a mean
 155 drainage basin area of 0.7 km² (Table 1). The results of this ensemble of simulations are
 156 presented in Figure 1 where we show the evolution of the surface velocity and effective
 157 pressure as a mean value over the whole domain and at given altitudes.

158 The mean velocity over the domain (Figure 1a) presents a typical pattern for a glacier
 159 with a marked and short-lived spring speed-up event followed by a second acceleration
 160 event before the velocities drop down to a lower level. At the end of the melt season we
 161 see a large spread in the evolution of the velocities with some of the ensemble members
 162 showing a strong re-acceleration while other tend to stay at a more reasonable summer
 163 velocity level. The velocity patterns are driven by the evolution of the effective pressure,
 164 as shown on Figure 1f the initial speed up is related to a sharp drop in effective pres-
 165 sure at the beginning of the melt season. Then the activation of the efficient drainage
 166 system leads to a gentler slope in the decrease of the effective pressure which in turn al-
 167 lows the velocity to slow down to their summer level. Finally at the end of the season,
 168 the end of the melt leads to a fast increase of the effective pressure which is mediated
 169 by the pace at which the efficient drainage system collapses and explains why some mem-

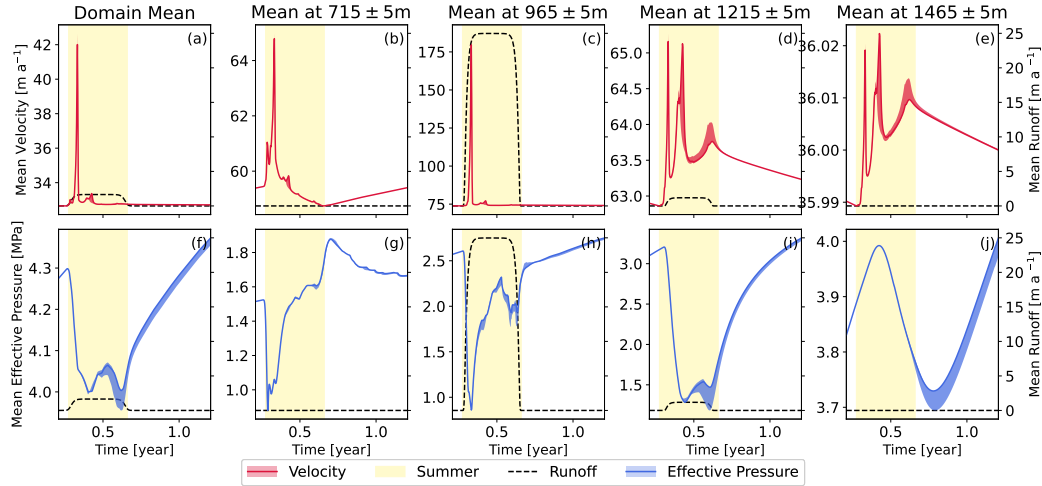


Figure 2. Same as Figure 1 but for the *Coarse* ensemble. Note that the runoff is null at 715 m as there is no moulines in this elevation band

170 bers have a strong end of summer acceleration while other don't. The velocity and ef-
 171 fective pressure pattern is quite different depending on the altitude that we consider. At
 172 low elevations (below 1000m, Figures 1b-c and 1g-h) the velocity and effective pressure
 173 evolution are very similar to the one described for the whole domain with a slight dif-
 174 ference in the fact that the effective pressure rebounds to slightly higher values once the
 175 efficient drainage system is activated. At higher elevation but below the no melt zone
 176 (Figures 1d and i) the most obvious change is the absence of a spring speed-up event.
 177 At this elevation, the velocity evolution is characterised by a gradual increase in vel-
 178 ocities from the beginning of the melt season all the way to its end. This acceleration is
 179 driven by a decrease in effective pressure that first drops at the beginning of the melt
 180 season and then levels out but without the rebound that was observed at lower eleva-
 181 tions. Above the melt region (Figures 1e and j) the velocity pattern is similar as described
 182 above but with a much smaller amplitude (note the changes in y-axis range in Figure 1).
 183 Here the small amplitude of the velocity changes, the decoupling with the effective pres-
 184 sure evolution, and the absence of meltwater input points towards a velocity change that
 185 is due to the downstream evolution of velocities.

186 Changing the number of moulines that are used to inject water into the subglacial
 187 drainage system as a large impact on the model results. Figure 2 shows the result for
 188 the *Coarse* simulation with only 50 moulines which translates to a mean catchment area
 189 of 13 km² (Table 1).

190 The first obvious difference with Figure 1 is the drastically smaller amplitude of
 191 the velocity changes for the simulation with a lower number of moulines. An other clear
 192 result is the diminution in the spread of the computed velocities with the ensemble with
 193 only 50 moulines showing almost no spread between its members (Figure 2). The reduc-
 194 tion of the number of moulines as presented on the *Coarse* simulation (Figure 2) leads
 195 to the disappearance of the end of summer acceleration at all elevations. The velocity
 196 response of the *Coarse* simulation is entirely explained by the changes in the evolution
 197 of the effective pressure during the melt season. While the evolution at higher altitudes
 198 is quite comparable for the *Uniform* (Figure 1i-j) and *Coarse* (Figure 2i-j) simulations
 199 the patterns are quite different at lower elevations. Closer to the glacier front, the ef-
 200 fective pressure of the *Coarse* simulations (Figure 2g-h) show an earlier rebound of the pres-
 201 sures towards a higher summer value after the initial drop than the one in the *Uniform*

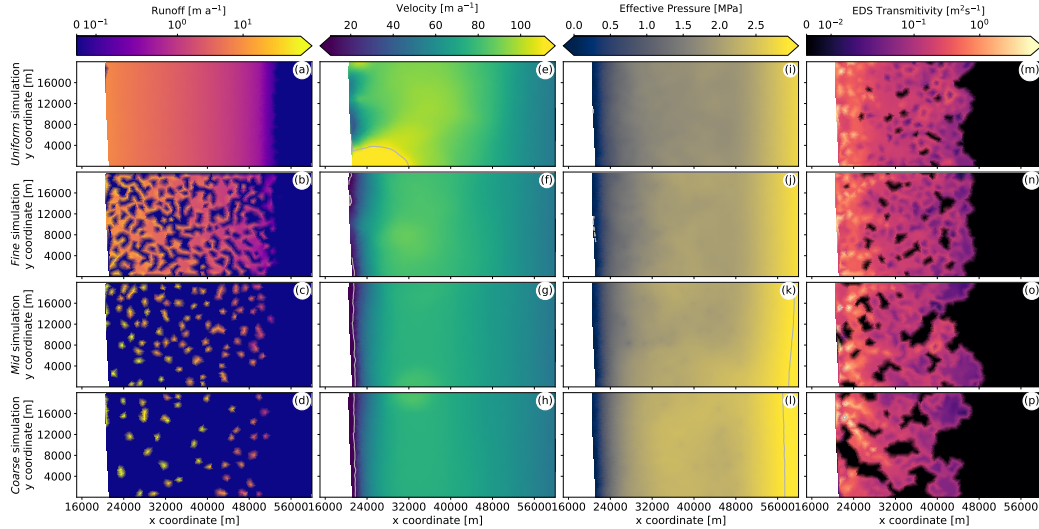


Figure 3. Annual mean values of Runoff (a-d), Velocity (e-h), Effective Pressure (i-l) and efficient drainage system (EDS) Transmittivity (m-p) for the different simulations (*Uniform*, *Fine*, *Mid*, *Coarse*). The ice flow is from right to left and we only show here the lower region of the glacier which experiences melt. The grey lines show the boundaries out of which the colorbar is saturated. We present here the values for a single member of the ensemble and all other ensemble members show a similar pattern.

202 ensemble (Figure 1g-h). It is this difference in effective pressure that explains why the
 203 end of summer acceleration events are mostly absent from the simulations with a smaller
 204 number of moulins.

205 A map view of the mean annual value of the different variables of the model give
 206 a better insight into the sources of the differences that are observed in the effective pres-
 207 sure and velocity evolution. Figure 3 presents map views of the region of the glacier where
 208 the runoff takes place leaving out the uppermost region of the glacier where the differ-
 209 ences due to a change in recharge distribution are less pronounced.

210 Figure 3 compares the mean annual runoff, velocity, effective pressure and efficient
 211 drainage system transmittivity for a given member of the four ensembles from *Uniform*
 212 at the top to *Coarse* at the bottom. Note here that as the number of moulins reduces,
 213 the intensity of the recharge at each of those points increase as the moulins are drain-
 214 ing a larger area of the glacier and so funnelling a larger amount of water toward the ice
 215 base (see Table 1 for statistics on catchment area). In term of velocities Figures 3(e-h)
 216 show the large difference that appears between the simulation fed by every node or the
 217 ones that receive water through a decreasing number of moulins that was already shown
 218 on Figures 1 and 2. The observation of the temporal evolution of velocities are confirmed
 219 by the mean annual values with notably faster velocities if the water input is spread over
 220 a larger number of moulins. The upstream shift of the maximum velocity region which
 221 was noticeable on the temporal evolution is also very clear here with only the *Uniform*
 222 simulation that presents its fastest velocity towards the front of the glacier while the sim-
 223 ulation with a lower number of moulins have their maximum velocities roughly 12km up-
 224 stream from the front. This is driven by the effective pressure presented on Figures 3(i-
 225 l) where we observe higher effective pressure with a lower number of moulins but also
 226 a more grainy pattern for the effective pressure which is driven by the coarser water in-
 227 put. Those fields are explained by the way in which the efficient drainage system devel-

ops, on Figures 3(m-p) we show the mean transmissivity of the efficient drainage system which describes its efficiency. We see for the *Uniform* simulation a smooth transmissivity pattern for the efficient drainage system with a decrease from high efficiency at the front to lower efficiency at the top of the ablation zone. As the number of moulins is reduced the efficient drainage system shows a more localised pattern where the regions of the efficient drainage system that are active are also more efficient than they were when a large area of the bedrock was occupied by the efficient drainage system.

4 Discussion

Our experiments show that the distribution of injection points to the subglacial drainage system leads to substantial changes in both the geometry of the efficient drainage system and its overall impact on ice velocity.

This conclusion is in line with the study Scholzen et al. (2021) that showed that a more localised water input into the subglacial drainage system leads to a faster development of the efficient subglacial drainage system. It is however quite different from the results presented by A. Banwell et al. (2016) who found that a higher moulin density causes an earlier onset of channelization and overall more widespread efficient drainage system. We argue that the differences here are mostly due to the change in timing in their recharge scenario but also on the definition of the efficient drainage. A. Banwell et al. (2016) consider any channel that opens as an efficient drainage system, but looking at their Figure 4 we see that their simulations present the same patterns as ours with a lower moulin density leading to less widespread efficient drainage system but with a higher efficiency. This leads to a more efficient drainage of the inefficient drainage system and higher effective pressures which in turns causes slower ice flow than in experiments with a more homogeneous water recharge.

In our model, the specific localisation of water input induces a more stable configuration of the subglacial drainage system. This is due to the fact that the moulins act as anchor points for the subglacial drainage system to develop. This contrasts with the more random development of the efficient drainage system for simulations with a more uniform input which lead to large spread of effective pressure within a given model ensemble (see *Uniform* ensemble and simulations from (de Fleurian et al., 2022)).

The observed response can be compared to the results of our preceding study comparing the intensity vs. length of the melt season (de Fleurian et al., 2022). There, a more intense melt season was driving a slower ice flow as it allowed the faster development of the efficient drainage system and as such an overall higher effective pressure. That compares well with the results that we show here, were a lower number of moulins lead to a more intense and localised water input. This triggers a faster development of the efficient drainage system at these locations which help to raise the effective pressure on the whole domain and such lead to a slower glacier.

The change in the distribution of the water sources also shows an upstream shift in the maximum velocity values. This is well illustrated in Figures 3(e-h) but also comparing the velocities on Figures 1, S1, S2, and 2 where we see an upstream migration of the fastest velocities. The pattern of the lower density moulin simulations are more coherent with the velocity patterns that have been observed in Greenland (Fitzpatrick et al., 2013; Sole et al., 2013). This change is driven by the concentration of subglacial water in a small number of pathways at the front of the glacier. The large efficiency of the drainage system close to the front leads to a quick rebound of the effective pressure at the beginning of summer towards a high effective pressure. This, in turns, reduces the intensity of the spring speed-up for the simulations with a low moulin density (*Mid* and *Coarse*). The recurrence of late summer acceleration is also reduced when the water input is achieved through a network of moulins rather than a uniform input. Again that

278 is due to the localisation of the water input which leads to more localised and efficient
 279 subglacial drainage system. Those well developed system tend to be active longer through
 280 the season and avoids the low effective pressure that was observed with more widespread
 281 water input.

282 5 Conclusions

283 On a synthetic geometry and with an idealised meltwater forcing, we show that a
 284 change in the distribution of the meltwater input to the basal drainage system as a large
 285 impact on the velocity of the overlying glacier. Our experiments show that as the num-
 286 ber of moulins diminishes, and the intensity of the recharge at these points increases, the
 287 velocity at the surface of the glacier greatly decreases. We associate this decrease in ve-
 288 locity to a faster, and more localised development of the efficient drainage system in our
 289 model with a higher efficiency of this system. The more localised water input into the
 290 subglacial hydrology model also leads in this particular model to a better physical sta-
 291 bility of the model due to the “anchoring” effect of the more localised input which con-
 292 strains the location of the efficient drainage system. The results of this study show the
 293 importance of moving away from uniform water input into subglacial hydrology mod-
 294 els. This poses the question of what is the real distribution of moulins and warrants more
 295 studies to allow a better characterisation of the supraglacial drainage system that would
 296 be usable for subglacial hydrology models.

297 Open Research Section

298 The Ice-sheet and Sea-level System Model is freely available at [https://issm.jpl](https://issm.jpl.nasa.gov/)
 299 [.nasa.gov/](https://issm.jpl.nasa.gov/) this specific study uses the development branch of the code at the revision
 300 number 27528 last updated on January 19 2023. The model set-up, outputs and post
 301 treating scripts corresponding to this study are available on zenodo (doi to come). The
 302 figures in this manuscript were generated with the script in the archive above and with
 303 Matplotlib v3.5 (Hunter, 2007).

304 Acknowledgments

305 This work is part of the SWitchDyn project funded by the Research Council of Norway
 306 (NFR-287206). Computing was performed on the resources provided by UNINETT Sigma2
 307 – the National Infrastructure for High Performance Computing and Data Storage in Nor-
 308 way (NN9635K and NS9635K).

309 References

- 310 Andrews, L. C., Catania, G. A., Hoffman, M. J., Gulley, J. D., Luethi, M. P., Ryser,
 311 C., ... Neumann, T. A. (2014). Direct observations of evolving subglacial
 312 drainage beneath the greenland ice sheet. *Nature*, *514*(7520), 80+. doi:
 313 10.1038/nature13796
- 314 Banwell, A., Hewitt, I., Willis, I., & Arnold, N. (2016). Moulin density controls
 315 drainage development beneath the Greenland ice sheet. *J.Geophys. Res.*,
 316 *121*(12), 2248–2269. doi: 10.1002/2015JF003801
- 317 Banwell, A. F., Arnold, N. S., Willis, I. C., Tedesco, M., & Ahlstrøm, A. P. (2012).
 318 Modeling supraglacial water routing and lake filling on the greenland ice
 319 sheet. *Journal of Geophysical Research: Earth Surface*, *117*(F4). doi:
 320 10.1029/2012JF002393
- 321 Bartholomew, I., Nienow, P., Mair, D., Hubbard, A., King, M. A., & Sole, A. (2010).
 322 Seasonal evolution of subglacial drainage and acceleration in a Greenland
 323 outlet glacier. *Nat. Geosci.*, *3*(6), 408–411. doi: 10.1038/NGEO863
- 324 Bartholomew, I., Peter, N., Andrew, S., Douglas, M., Thomas, C., & A., K. M.

- 325 (2012). Short-term variability in greenland ice sheet motion forced by time-
 326 varying meltwater drainage: Implications for the relationship between sub-
 327 glacial drainage system behavior and ice velocity. *J. Geophys. Res.*, *117*(F3).
 328 doi: 10.1029/2011JF002220
- 329 Chandler, D. M., Wadhwa, J. L., Lis, G. P., Cowton, T., Sole, A., Bartholomew, I.,
 330 ... Hubbard, A. (2013). Evolution of the subglacial drainage system beneath
 331 the Greenland Ice Sheet revealed by tracers. *Nat. Geosci.*, *6*(3), 195–198. doi:
 332 10.1038/ngeo1737
- 333 Clason, C., Mair, D. W. F., Nienow, P. W., Bartholomew, I. D., Sole, A., Palmer,
 334 S., & Schwanghart, W. (2015). Modelling the transfer of supraglacial meltwa-
 335 ter to the bed of leverett glacier, southwest greenland. *The Cryosphere*, *9*(1),
 336 123–138. doi: 10.5194/tc-9-123-2015
- 337 Colgan, W., Steffen, K., McLamb, W. S., Abdalati, W., Rajaram, H., Motyka,
 338 R., ... Anderson, R. (2011). An increase in crevasse extent, west green-
 339 land: Hydrologic implications. *Geophys. Res. Lett.*, *38*, L18502, 1–7. doi:
 340 10.1029/2011GL048491
- 341 Davison, B. J., Sole, A. J., Livingstone, S. J., Cowton, T. R., & Nienow, P. W.
 342 (2019). The influence of hydrology on the dynamics of land-terminating sectors
 343 of the greenland ice sheet. *Front. Earth Sci.*, *7*. doi: 10.3389/feart.2019.00010
- 344 de Fleurian, B., Davy, R., & Langebroek, P. M. (2022). Impact of runoff temporal
 345 distribution on ice dynamics. *The Cryosphere*, *16*(6), 2265–2283. doi: 10.5194/
 346 tc-16-2265-2022
- 347 de Fleurian, B., Gagliardini, O., Zwinger, T., Durand, G., Le Meur, E., Mair, D.,
 348 & Råback, P. (2014). A double continuum hydrological model for glacier
 349 applications. *The Cryosphere*, *8*(1), 137–153. doi: 10.5194/tc-8-137-2014
- 350 de Fleurian, B., Morlighem, M., Seroussi, H., Rignot, E., van den Broeke, M. R.,
 351 Munneke, P. K., ... Tedstone, A. J. (2016). A modeling study of the ef-
 352 fect of runoff variability on the effective pressure beneath russell glacier, west
 353 greenland. *J. Geophys. Res.*, *121*(10). doi: 10.1002/2016JF003842
- 354 Doyle, S. H., Hubbard, A., Fitzpatrick, A. A. W., van As, D., Mikkelsen, A. B., Pet-
 355 tersson, R., & Hubbard, B. (2014). Persistent flow acceleration within the
 356 interior of the greenland ice sheet. *Geophys. Res. Lett.*, *41*(3), 899–905. doi:
 357 10.1002/2013GL058933
- 358 Fitzpatrick, A. A. W., Hubbard, A., Joughin, I., Quincey, D. J., Van As, D.,
 359 Mikkelsen, A. P. B., ... Jones, G. A. (2013). Ice flow dynamics and sur-
 360 face meltwater flux at a land-terminating sector of the greenland ice sheet. *J.*
 361 *Glaciol.*, *59*(216), 687–696. doi: 10.3189/2013JoG12J143
- 362 Gagliardini, O., Cohen, D., Raback, P., & Zwinger, T. (2007). Finite-element mod-
 363 eling of subglacial cavities and related friction law. *J. Geophys. Res.*, *112*(F2),
 364 1–11. doi: 10.1029/2006JF000576
- 365 Gagliardini, O., & Werder, M. A. (2018). Influence of increasing surface melt over
 366 decadal timescales on land-terminating greenland-type outlet glaciers. *J.*
 367 *Glaciol.*, *64*(247), 1–11. doi: 10.1017/jog.2018.59
- 368 Glen, J. (1958). The flow law of ice: A discussion of the assumptions made in glacier
 369 theory, their experimental foundations and consequences. *IASH Publ.*, *47*, 171–
 370 183.
- 371 Hewitt, I. J. (2013). Seasonal changes in ice sheet motion due to melt water lubrication.
 372 *Earth Planet. Sci. Lett.*, *371–372*(0), 16–25. doi: 10.1016/j.epsl.2013.04
 373 .022
- 374 Hoffman, M., & Price, S. (2014). Feedbacks between coupled subglacial hydrology
 375 and glacier dynamics. *J. Geophys. Res.*, *119*(3), 414–436. doi: 10.1002/
 376 2013JF002943
- 377 Hoffman, M. J., Perego, M., Price, S. F., Lipscomb, W. H., Zhang, T., Jacobsen, D.,
 378 ... Bertagna, L. (2018). Mpas-albany land ice (mali): a variable-resolution
 379 ice sheet model for earth system modeling using voronoi grids. *Geosci. Model*

- 380 *Dev.*, 11(9), 3747–3780. doi: 10.5194/gmd-11-3747-2018
- 381 Hunter, J. D. (2007). Matplotlib: A 2d graphics environment. *Computing in Science*
- 382 *& Engineering*, 9(3), 90–95. doi: 10.1109/MCSE.2007.55
- 383 Iken, A. (1981). The effect of the subglacial water pressure on the sliding velocity of
- 384 a glacier in an idealized numerical model. *J. Glaciol.*, 27(97), 407–421.
- 385 Larour, E., Seroussi, H., Morlighem, M., & Rignot, E. (2012). Continental
- 386 scale, high order, high spatial resolution, ice sheet modeling using the Ice
- 387 Sheet System Model (ISSM). *J. Geophys. Res.*, 117(F01022), 1–20. doi:
- 388 10.1029/2011JF002140
- 389 MacAyeal, D. (1989). Large-scale ice flow over a viscous basal sediment: Theory and
- 390 application to Ice Stream B, Antarctica. *J. Geophys. Res.*, 94(B4), 4071–4087.
- 391 Meierbachtol, T., Harper, J., & Humphrey, N. (2013). Basal drainage system
- 392 response to increasing surface melt on the greenland ice sheet. *Science*,
- 393 341(6147), 777–779. doi: 10.1126/science.1235905
- 394 Mejia, J. Z., Gulley, J. D., Trunz, C., Covington, M. D., Bartholomew, T. C.,
- 395 Breithaupt, C., ... Dixon, T. H. (2022). Moulin density controls the
- 396 timing of peak pressurization within the greenland ice sheet’s subglacial
- 397 drainage system. *Geophysical Research Letters*, 49(22), e2022GL100058.
- 398 doi: 10.1029/2022GL100058
- 399 Morland, L., & Zainuddin, R. (1987). Plane and radial ice-shelf flow with prescribed
- 400 temperature profile. In Veen, C.J. van der, and Oerlemans, J., eds. *Dynamics*
- 401 *of the West Antarctica Ice Sheet. Proceedings of a Workshop held in Utrecht,*
- 402 *May 6-8, 1985. Dordrecht, D. Rediel Publishing Company*, 117(40), 117-140.
- 403 Pimentel, S., Flowers, G. E., & Schoof, C. G. (2010). A hydrologically coupled
- 404 higher-order flow-band model of ice dynamics with a Coulomb friction sliding
- 405 law. *J. Geophys. Res.*, 115, 1–16. doi: 10.1029/2009JF001621
- 406 Scholzen, C., Schuler, T. V., & Gilbert, A. (2021). Sensitivity of subglacial
- 407 drainage to water supply distribution at the kongsfjord basin, svalbard. *The*
- 408 *Cryosphere*, 15(6), 2719–2738. doi: 10.5194/tc-15-2719-2021
- 409 Schoof, C. (2005). The effect of cavitation on glacier sliding. *Proc. R. Soc. A*,
- 410 461(2055), 609–627. doi: 10.1098/rspa.2004.1350
- 411 Schoof, C. (2010). Ice-sheet acceleration driven by melt supply variability. *Nature*,
- 412 468(7325), 803–806. doi: 10.1038/nature09618
- 413 Sole, A., Nienow, P., Bartholomew, I., Mair, D., Cowton, T., Tedstone, A., & King,
- 414 M. A. (2013). Winter motion mediates dynamic response of the greenland
- 415 ice sheet to warmer summers. *Geophys. Res. Lett.*, 40(15), 3940–3944. doi:
- 416 10.1002/grl.50764
- 417 Stevens, L. A., Hewitt, I. J., Das, S. B., & Behn, M. D. (2018). Relationship be-
- 418 tween greenland ice sheet surface speed and modeled effective pressure. *Jour-*
- 419 *nal of Geophysical Research: Earth Surface*, 123(9), 2258–2278. doi: 10.1029/
- 420 2017JF004581
- 421 Tedesco, M., Willis, I. C., Hoffman, M. J., Banwell, A. F., Alexander, P., &
- 422 Arnold, N. S. (2013). Ice dynamic response to two modes of surface lake
- 423 drainage on the Greenland ice sheet. *Environ. Res. Lett.*, 8(3), 034007. doi:
- 424 10.1088/1748-9326/8/3/034007
- 425 Tedstone, A. J., Nienow, P. W., Gourmelen, N., Dehecq, A., Goldberg, D., &
- 426 Hanna, E. (2015). Decadal slowdown of a land-terminating sector of the
- 427 greenland ice sheet despite warming. *Nature*, 526(7575), 692–695. doi:
- 428 10.1038/nature15722
- 429 van de Wal, R. S. W., Smeets, C. J. P. P., Boot, W., Stoffelen, M., van Kampen, R.,
- 430 Doyle, S. H., ... Hubbard, A. (2015). Self-regulation of ice flow varies across
- 431 the ablation area in south-west greenland. *The Cryosphere*, 9(2), 603–611. doi:
- 432 10.5194/tc-9-603-2015
- 433 Werder, M. A., Hewitt, I. J., Schoof, C. G., & Flowers, G. E. (2013). Modeling
- 434 channelized and distributed subglacial drainage in two dimensions. *J. Geophys.*

- 435 *Res.*, 118, 1–19. doi: 10.1002/jgrf.20146
- 436 Yang, K., Smith, L. C., Andrews, L. C., Fettweis, X., & Li, M. (2022). Supraglacial
437 drainage efficiency of the greenland ice sheet estimated from remote sens-
438 ing and climate models. *J. Geophys.Res.*, 127(2), e2021JF006269. doi:
439 10.1029/2021JF006269
- 440 Yang, K., Sommers, A., Andrews, L. C., Smith, L. C., Lu, X., Fettweis, X., & Li,
441 M. (2020). Intercomparison of surface meltwater routing models for the green-
442 land ice sheet and influence on subglacial effective pressures. *The Cryosphere*,
443 14(10), 3349–3365. doi: 10.5194/tc-14-3349-2020
- 444 Zwally, H. J., Abdalati, W., Herring, T., Larson, K., Saba, J., & Steffen, K. (2002).
445 Surface melt-induced acceleration of Greenland ice-sheet flow. *Science*,
446 297(5579), 218–222. doi: 10.1126/science.1072708